J Appl Electrochem (2009) 39:2385–2395
DOI 10.1007/s10800-009-9925-z

ORIGINAL PAPER

# Organosilanes and polypyrrole as anticorrosive treatment of aluminium 2024

**A. L. Correa-Borroel · S. Gutierrez · E. Arce · R. Cabrera-Sierra · P. Herrasti**

Received: 22 December 2008 / Accepted: 29 April 2009 / Published online: 21 May 2009


**Abstract** This paper addresses the preparation and characterisation of anticorrosive silane- and polypyrrole-based organic coatings and combinations of the two on aluminium 2024. Layer adsorption studies of organosilanes such as propyl (C3), octyl (C8) and octadecyl (C18) trimethoxysilane and polypyrrole deposits on the aluminium electrodes reveal only limited protection. Their anticorrosive power declines when they are subject to highly corrosive environments, such as salt fog cabinets, for extended periods. The combination of both deposits yields a more protective structure that affords better protection with time. The best performance is achieved with polypyrrole deposits on silanes due to the excellent bonding between the silane adsorbed on the surface of the material and the polypyrrole film. Of the three organosilanes used, the one with the shortest chain performs best. When long-chain organosilanes are used, the polypyrrole film becomes detached due to the lesser interaction between the layers. Electrochemical impedance spectroscopy and morphological studies of the layers also show the greater adhesion and lesser deterioration of polypyrrole deposits on silane layers.

**Keywords** Aluminium · Organic coatings · Organosilanes · Polypyrrole · Corrosion

A. L. Correa-Borroel · P. Herrasti (✉)
Facultad de Ciencias, Universidad Autónoma de Madrid, Cantoblanco s/n, 28049 Madrid, Spain
e-mail: pilar.herrasti@uam.es

A. L. Correa-Borroel · S. Gutierrez
IIC, Universidad de Guanajuato, Cerro de la Venada S/N, Gto., Guanajuato 36040, CP, México

E. Arce
Departamento de Ingeniería Metalúrgica, IPN-ESIQIE, UPALM Ed 7, 07738 México, DF, México

R. Cabrera-Sierra
Departamento de Ingeniería Química, IPN-ESIQIE, UPALM Ed 7, 07738 México, DF, México

## 1 Introduction

Aluminium is a very widely used metal which, despite its oxide layer, can deteriorate in strongly corrosive environments. This has led to a great number of studies on the prevention or minimisation of Al oxidation. The most widespread pretreatment for aluminium protection is the use of chromate baths. However, due to the well-known environmental and health problems generated by Cr(VI) [1], attempts are being made to develop other less aggressive methods, such as organic coatings.

Among the different types of organic coatings, conducting polymers offer several benefits and have been widely studied [2–8]. These polymers behave as a protective layer, but in many cases present adhesion problems and need a promoter to facilitate their interaction with the metal surface to be protected. This may be achieved with organosilanes, which bond to the metallic oxide and serve as an intermediary to fix other types of coatings such as polypyrrole.

Organofunctional silanes are hybrid organic–inorganic compounds that can be used to couple agents through the organic–inorganic interface. The general structure is of the type $X_3Si(CH_2)_nY$, where X may be a methoxy or ethoxy group, capable of hydrolysing, and Y is an organofunctional group such as a chorine, amine, epoxy or mercaptan. Plueddemann [9] suggested that organofunctional silanes can bond to the surface of a metal via the formation of an

oxane bond (Me-O–Si). This bond is induced by the interaction of the silanol groups (Si–OH) with the hydroxide groups of the metal surface. The reaction may be expressed as:

$$Me-OH + H-O-Si \rightarrow Me-OH-Si + H_2O$$

Organosilane films are widely recognised as barrier coatings to water [10–12], thanks to their hydrophobia, and act as a physical barrier against corrosion. If the deposit is obtained in appropriate conditions their effect has certain durability, but it is also known that Me–O–Si bonds can hydrolyse and thus lose their hydrophobic and protective properties [13].

One way to increase the robustness and thickness of the layer is by the inclusion of additives in the silane deposits, such as silica or alumina nanoparticles [14, 15] or inhibitors [16, 17]. Although these new methods have achieved some improvement compared to just silane films, new formulations are required in order to raise the durability of their anticorrosive power.

The electrodeposition of conducting polymers is another possible strategy to prevent the corrosion of a metal. One of the most widely used conducting polymers is polypyrrole (Ppy), which may be synthesised by chemical or electrochemical deposition, although the latter technique yields films of greater conductivity. The deposit acts in two ways: as a physical barrier, and to maintain the passive properties of metals due to its redox properties. However, the oxidation potential of pyrrole (or other monomers such as aniline and thiophene, among others) is above the transpassivation potential of metals such as steel, aluminium and copper, giving rise to simultaneous oxidation of the metal and of the monomer. The literature includes a large number of studies of these materials as anticorrosive deposits [18–22], but in many cases they present poor adhesion to the substrate and high porosity. In view of the problems experienced individually by each layer, the idea arose to use them in combination, on the one hand using a silane layer as an intermediate layer for the polymer, and on the other hand adsorbing a silane layer on a previously generated polypyrrole film. Thus, the proposal of this study is to combine both materials on aluminium alloy 2024 (AA2024) and compare the protective effect achieved with the individual layers.

## 2 Experimental

### 2.1 Preparation of organosilane layer (AA2024/silanes)

Three types of organosilanes were used: propyltrimethoxysilane (C3), octyltrimethoxysilane (C8) and octadecyltrimethoxysilane (C18); all of them pure Aldrich liquid products. The working electrode consisted of an aluminium 2024, AA2024 specimen (composition: 0.2% Si, 0.26% Fe, 4.5% Cu, 0.62% Mn, 1.33% Mg, 0.04% Zn, 0.05% Ti, 0.01% Pb, 0.01% Cr and 92.5% Al) with a surface area of 2 $cm^2$. The silanes were hydrolysed to form sufficient Si–OH groups. Hydrolysis was performed in the presence of water and methanol (silane/water/methanol 10/10/80%). The solution was vigorously stirred for 24 h. In the case of C3 and C8, pH was adjusted to 4 with acetic acid and, for C18, pH was adjusted to 8 with sodium hydroxide. The temperature was held at a constant 25 °C, and the solutions were prepared each time they were used.

Prior to the deposition of the silane film, the surface of the aluminium alloys was electrochemically treated to form a porous oxide film by the application of a 20 mA current for 350 s in a 0.3 M oxalic acid solution. The specimens were then submerged in the silane solution for 1 h and subsequently thermally treated for 1 h at 80 °C. This treatment was necessary to achieve condensation of the hydrolysed organosilane on the surface and its adhesion though with the formation of Al–O–Si bonds.

### 2.2 Preparation of polypyrrole (AA2024/Ppy)

Prior to the deposition of the Ppy film, the AA2024 specimen was polished with emery paper, washed with distilled water and degreased with acetone. The polypyrrole film was then electrodeposited by cyclic voltammetry using the specimen as the working electrode, which, in turn, was introduced into a stainless steel cell acting as counter electrode, and employing an Ag/AgCl (3 M) reference electrode. 0.1 M of nitric acid solution was used as the background electrolyte. Pyrrole (Aldrich), at a concentration of 0.5 M in all cases, was distilled and then kept in a refrigerator. Potential was varied from −0.2 to 1.4 V/Ag/AgCl (3 M) at a scanning rate of 100 mV $s^{-1}$, and the number of potential scan cycles was 40. A PAR Vstat potentiostat was used.

### 2.3 Preparation of bilayer (AA2024/silane/Ppy)

After forming the silane layer on the AA2024 surface, the Ppy film was electrodeposited under the same conditions indicated in Sect. 2, but applying only three potential cycles. The potential was varied from 0 to 1.4 V/Ag/AgCl (3 M) at a scan rate of 10 mV $s^{-1}$.

### 2.4 Preparation of bilayer (AA2024/Ppy/silane)

For the preparation of these bilayers, a Ppy layer was deposited according to the method described in Sect. 2, and a silane layer was adsorbed upon this using the same

dissolution, immersion time and curing time specified in Sect. 1.

### 2.5 Morphological characterisation of deposits

The morphology of the deposits was examined with a Phillips XL30EDAX PV 9900 scanning electron microscope.

### 2.6 Anticorrosive experiments

All electrochemical measurements were performed with a PAR VerSat. The cell used was a conventional three-electrode set-up with a stainless steel cell acting as counter electrode and an Ag/AgCl (3 M) reference electrode to which all potentials are referred. The working electrodes were the previously modified AA2024 specimens. The area exposed to the test solution (3% NaCl) was 2 $cm^2$. Anodic and cathodic polarisation curves were recorded separately in the positive and negative direction by scanning the potential from open circuit potential at a scanning rate of 2 mV $s^{-1}$. EIS measurements were taken with an Autolab 30 potentiostat, using the AC signal of the impedance measurements at the corrosion potential. The measured frequency range was from $10^{-2}$ to $10^4$ Hz with amplitude of ±10 mV.

## 3 Results and discussion

### 3.1 Characterisation of the films

#### *3.1.1 Oxide layer on AA2024*

For hydrolysed silane to condense on the AA2024 surface forming Al–O–Si bonds, the metal surface must be coated with OH groups, for which the presence of an oxide layer ($Al_2O_3$) is necessary [23–25]. For this purpose, an $Al_2O_3$ layer of a controlled thickness was formed on the untreated aluminium surface (i.e. on the native layer of the same oxide), applying a current of 20 mA for 350 s in 0.3 M oxalic acid solution The potential-time curve obtained for the growth of this oxide is shown in Fig. 1.

At the start of the curve, there is a sharp increase in the potential with respect to time, followed by a constant rise in potential. After 150 s, the potential remains constant at a value of approximately 13 V/Ag/AgCl (3 M), which can be related with the formation of a porous $Al_2O_3$ layer on AA2024 [26, 27] partially hydrated given by the contribution of an hydroxide. The pore diameter, density and thickness of the oxide layer formed depend on the oxalic acid concentration, the temperature, and the oxidation current [28]. For the conditions in which the oxide layer was formed, the pore diameter was approximately 30 nm, calculated using SEM images of the specimen.

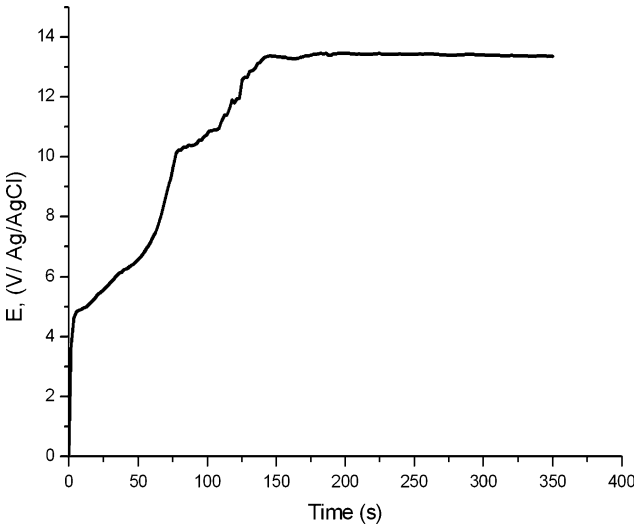


**Fig. 1** Voltage–time response for the anodising of aluminium in 0.3 M oxalic acid, applying 20 mA $cm^{-2}$

#### *3.1.2 AA2024/$Al_2O_3$/silanes*

The AA2024/$Al_2O_3$ surface was modified in the different silane solutions (C3, C8 and C18). Figure 2a shows a micrograph of the surface of an AA2024 specimen modified with a C3 silane layer obtained in 1 h of immersion and subsequently treated at 80 °C for 1 h. In this SEM image, it is possible to corroborate the homogeneity of the coating formed on the AA2024/$Al_2O_3$ surface. Moreover, the typical EDAX analysis performed on several areas of the surface, as shown in Fig. 2b, reveals the presence of Si. The same Si peak is observed in different areas of the coating, which could indicate that the substrate is completely covered by the organosilane. However, when the AA2024 was submerged for times of less than 1 h, the presence of Si was not observed on the entire surface, indicating that the films formed under these conditions were not homogeneous. Thus, the decision was made to prepare the silanes with an immersion time of 1 h.

#### *3.1.3 Al/$Al_2O_3$/silanes/Ppy layers*

Electrodeposition of the polymer required a prior experiment study to determine the conditions in which pyrrole oxidises. To induce the formation of polypyrrole on the AA2024, various electrochemical treatments can be used, i.e. potentiostatic and galvanostatic perturbations. However, the cyclic voltammetry technique allows for the generation of the best polymer layers—more homogeneous with adherent properties. Figure 3 shows voltagrams of polypyrrole deposition on the AA2024 surface (continuous line) and on the Al/silane surface (dashed line). Similar

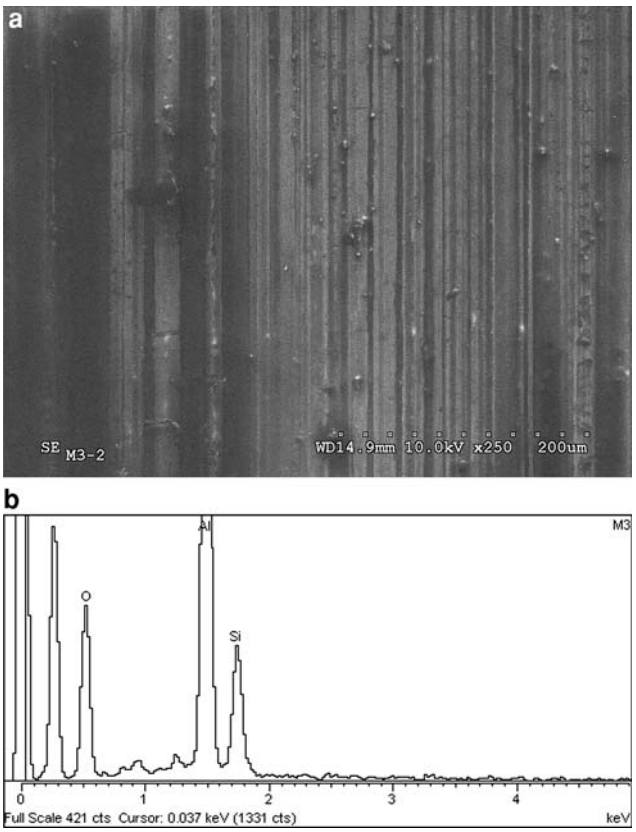


**Fig. 2** **a** SEM micrographs of the coated silane C3 on AA2024 and **b** EDAX of the surface after immersion in C3 for 1 h

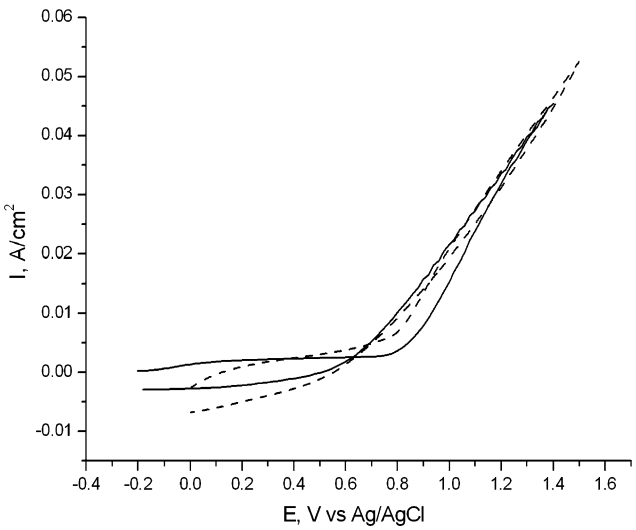


**Fig. 3** Cyclic voltammetry obtained on AA2024 (*thin line*) and AA2024/C3 (*dotted line*); in the first case, 40 cycles and $v = 100$ mV $s^{-1}$, and, in the second case, 3 cycles and $v = 10$ mV $s^{-1}$. In both cases, the solution was 0.5 M of pyrrole and 0.1 M $HNO_3$

voltagrams are obtained in both cases, in spite of the different surface conditions for each substrate, indicating that the silane coatings shown a certain degree of permeation of the aqueous solution. While 40 cycles are required to deposit Ppy with a thickness of 30 microns (an approximate calculation assuming that, in order to deposit 0.28 μm, 100 mC $cm^{-2}$ is needed [29]) and good adhesion on the AA2024, only 3 cycles at a scanning rate of 10 mV $s^{-1}$ are required to obtain approximately the same thickness on the silane. This fact, can be related with an increase of the geometric area of the AA2024, because the silane coating was formed on a rough surface (porous oxide–hydroxide) in comparison with a freshly polished surface of AA2024 for Ppy deposition. The case of polypyrrole on aluminium has been previously studied, showing that the best deposits are obtained on surfaces that present defects or imperfections on which the polymerisation process starts, growing along the entire substrate [7, 30]. No prior studies have been done on silanes, and we believe that the need for a lower number of cycles for electrodeposition is a consequence of a higher number of active zones over which the polymerisation will start, generating their collapse in a shorter time. Thus, a galvanostatic treatment was employed to favour the formation of an aluminium oxide with a porous nature and at the same time hydroxide ions for coupling the silane coating.

Electrodeposition of polypyrrole was only possible on thermally treated layers of silanes with very short preparation times. Silane layers exposed to air for time experienced degradation. This behaviour has been observed by other authors [13], who found that hydrolysis of the Al–Si–O bonds takes place, leading to a loss in adhesion to the substrate.

The Ppy films obtained in the above conditions were observed under the scanning electron microscope. The morphology of the polypyrrole films obtained on C3 silane is shown in Fig. 4, where is observed a typical granular

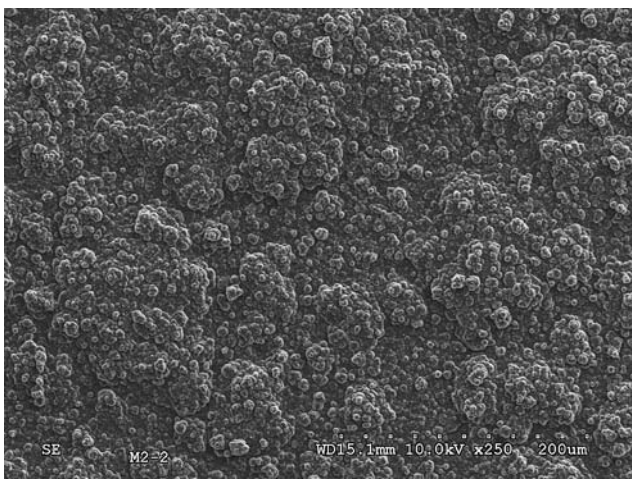


**Fig. 4** SEM micrograph of polypyrrole electrodeposited on aluminium substrate coated with C3 silane

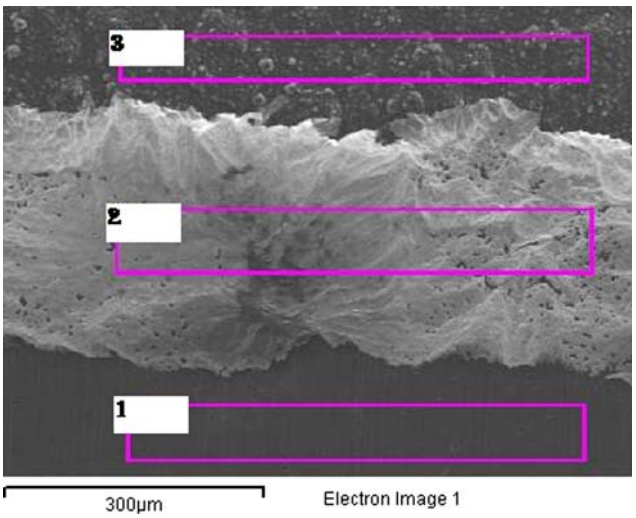


**Fig. 5** SEM micrograph showing the three different deposits: (1) AA2024/$Al_2O_3$, (2) C3, and (3) polypyrrole

structure of polypyrrole, although the grains are forming clusters. Figure 5 shows a micrograph of the film in which it is possible to see the AA2024 substrate with the oxide formed (zone 1), the silane layer (zone 2) and the polymer layer (zone 3). The film coating formed is not detached after the adhesion test performed with 3 M Scotch tape. This corroborates both the adhesion of the coatings on the AA2024 surface, and the homogeneous, low-porosity nature of the coatings.

### *3.1.4 AA2024/Ppy/silane*

The second strategy consisted of electrodepositing Ppy on the AA2024 surface and adsorbing silane layers onto this (AA2024/Ppy/silanes). To deposit Ppy in a nitric medium, it was necessary to polish the aluminium surface [18], since the presence of a fine oxide layer impedes electrodeposition (in contrast to the case of silanes). After the electrode has been polished, electropolymerisation takes place in the pitting zone, where small nuclei appear which collapse and grow to form a layer on the substrate [18]. Silane layers were adsorbed on this polymeric layer using the same methodology employed when they were adsorbed on the oxide layer. Adsorption, in this case, is probably due to the interaction of the hydrolysed silane's Si–OH group with the pyrrole's N–H group. Other authors [31] have reported that the interaction between organosilanes and polyaniline is probably due to the amine sites of the EB (emeraldine) and the amine group of the organosilane. In our case, the organosilane does not have this amino group, but the interaction can take place between the Si–OH group and the N–H group from the polypyrrole chain. This can explain why the interaction decreases when the silane chain is longer.

## 3.2 Corrosion behaviour

### *3.2.1 Potential–time curves*

Open-circuit potential measurements versus immersion time in a 3% NaCl solution were taken for AA2024, AA2024/silane, AA2024/silane/Ppy and AA2024/Ppy/silane substrates. These results are shown in Fig. 6. For AA2024 electrode is shown an important variation in the first 2,000 s, from −1 to −0.7 V vs. Ag/AgCl (3 M) (curve 1), which can be related with the formation of a porous oxide layer that covers the substrate; meanwhile, for longer immersion times the potential remains constant. When a silane layer is deposited on aluminium with an electrogenerated oxide layer (curve 2), its potential shifts slightly towards more positive values which can be related to the presence of the silane coating. Also, is observed that the potential remains almost constant after 5,000 s, suggesting no greater modifications of the AA2024/silane exposed to the solution. In contrast, the substrates that contain both silane/Ppy and Ppy/silane layers (curves 3 and 4) show a shift of the open circuit potential in the positive direction until reaching stabilisation, due to the relaxation of both systems in the electrolytic medium [32]. In both cases, the same potential of −0.5 V vs. Ag/AgCl (3 M) is achieved; i.e. 200 mV more positive than the value of AA2024 coated with the oxide layer. This higher potential, compared to AA2024 coated only with an oxide layer, indicates that both systems behave more nobly against the corrosion of the medium.

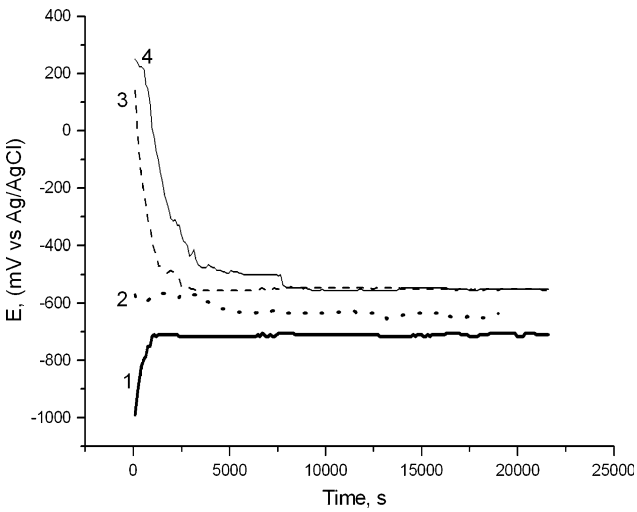


**Fig. 6** Open circuit potential versus immersion time in a 3% NaCl solution for substrates coated with silane, AA2024/silane/Ppy and AA2024/Ppy/silane: (1) AA2024 (*thick line*), (2) AA2024/C3 (*dots*), (3) AA2024/C3/Ppy (*dotted line*), (4) AA2024/Ppy/C3 (*thin line*)

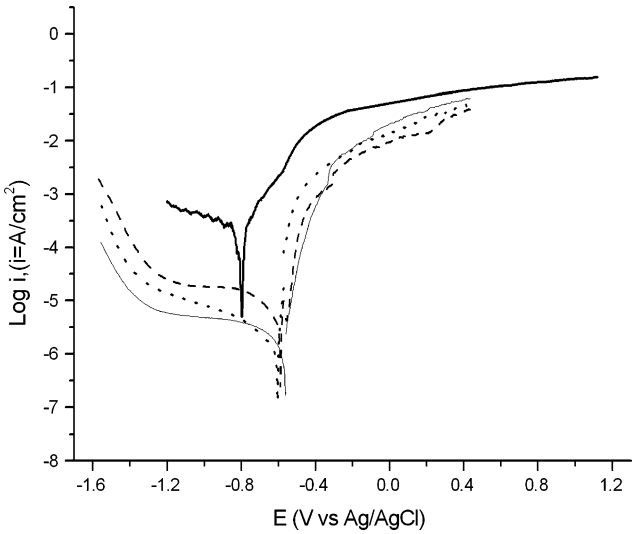


**Fig. 7** Polarisation curves obtained in 3% NaCl of the aluminium and the three silanes coating aluminium: AA2024/$Al_2O_3$ (*thick line*), AA2024/C3 (*dots*), AA2024/C8 (*dotted line*), AA2024/C18 (*thin line*)

### 3.2.2 Polarisation curves

Figure 7 shows polarisation curves obtained in 3% NaCl, for the three silanes (C3, C8 and C18) adsorbed on the oxide layer generated on AA2024 and the curve of aluminium. The corrosion potential shifts only slightly towards more positive values. This figure shows similar electrochemical behaviour for all cases, with the main difference being a decrease in the current magnitudes in presence of the silane coatings. This has also been observed in the case of other silanes [33]. In the cathodic branch, a typical response controlled by the diffusion of molecular oxygen is observed; meanwhile, reduction of water is observed at more negative potentials. In the anodic curve, active behaviour is evident, reaching a diffusion-controlled process at more positive potentials, probably related to the $Al^{3+}$ ions from the metal film interface through the oxide and coating. These modifications in the polarisation curves do not follow Tafel's equation, making it difficult to evaluate the corrosion rate using this approximation. The anodic and cathodic curves are seen to have the same shape, which clearly indicates that silanes act mostly as a physical barrier and do not interfere in the redox processes that take place.

To verify the stability of these films in the corrosive medium, they were subjected to the salt fog cabinet for 72 h or submerged for 7 days in a 3% NaCl solution. It is generally observed that the plates experienced deterioration. As an example, Fig. 8 shows the morphology of a AA2024/silane plate after 7 days of immersion, revealing the damage and detachment of the C3 silane layer in some regions of the surface. As was suggested above, the

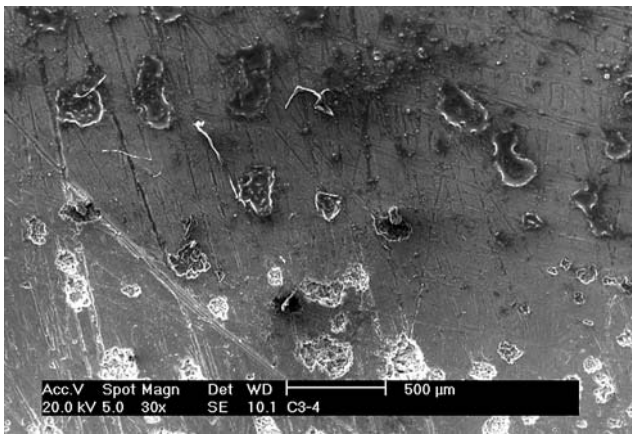


**Fig. 8** SEM micrographs obtained on an AA2024/C3 substrate after treatment in salt fog cabinet for 72 h

damage observed on the AA2024/silane can be related to the permeation of the aqueous solution through the silane coatings. The entrance of the aqueous solution favours the pitting of the AA2024 by the high concentration of chloride ions. However, it seems that the protective behaviour can be increased by coupling the polypyrrole film, if we consider that conducting polymers can act as chemical barriers to the corrosion process [34].

Polarisation curves were drawn for the AA2024/silane/Ppy substrates and are shown in Fig. 9. As can be seen, the corrosion potential of specimens with both layers shifts towards positive values, from −650 mV/Ag/AgCl (3 M) for the oxidised aluminium electrode to 300 mV/Ag/AgCl (3 M) when silanes C3 and C8 is used; meanwhile, a smaller shift is observed for C18 silane. The mechanism of

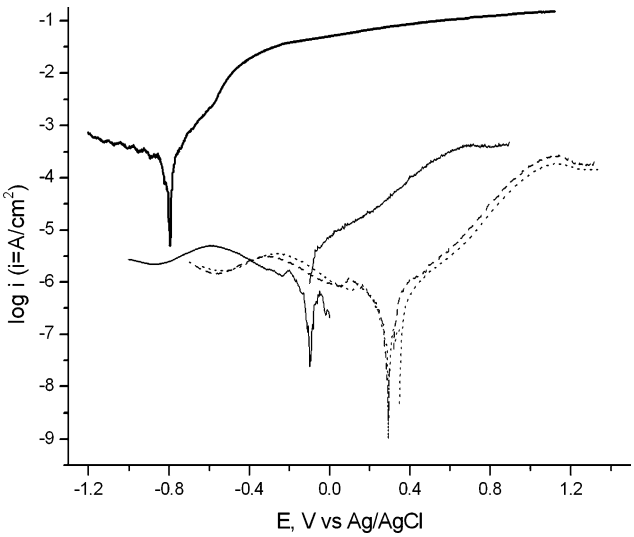


**Fig. 9** Polarisation curves obtained in 3% NaCl of the aluminium and polypyrrole electrodeposited on the three different silanes: AA2024/$Al_2O_3$ (*thick line*), AA2024/C3/Ppy (*dots*), AA2024/C8/Ppy (*dotted line*), AA2024/C18/Ppy (*thin line*)

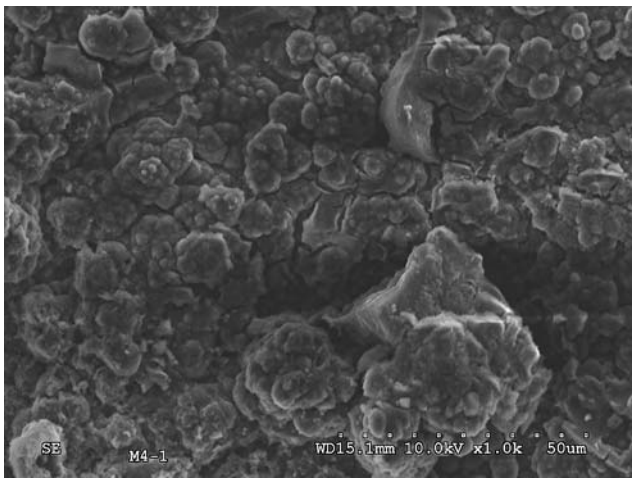


**Fig. 10** SEM micrograph obtained for AA2024/C3/Ppy after treatment in salt fog cabinet for 72 h

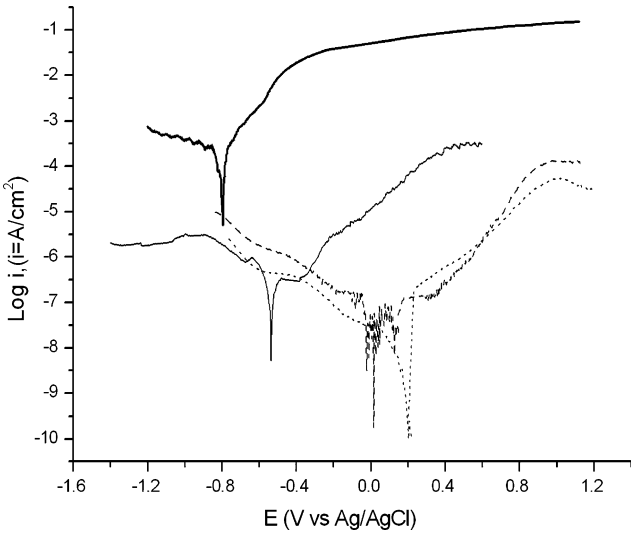


**Fig. 11** Polarisation curves obtained in 3% NaCl of the aluminium substrate and the different silanes adsorbed on aluminium with polypyrrole electrodeposited: AA2024/$Al_2O_3$ (*thick line*), AA2024/Ppy/C3 (*dots*), AA2024/Ppy/C8 (*dotted line*), AA2024/Ppy/C18 (*thin line*)

polymer electrodeposition over the silane layer has not been studied. However, it can be suggested that when the silane chain is long (such is the case for C18), the deposits are less homogeneous because the adsorption mechanism is influenced by the complex structure of the silane on the AA2024. The electrodeposition of Ppy can be less uniform and with poor adherence. It is noteworthy that in Fig. 9, the current magnitudes obtained for C3 and C8 silanes (AA2024/silane/Ppy) are lower in comparison with those evaluated for AA2024/silane (Fig. 7) [34]. To corroborate the protective properties of these coatings, their morphology after being subjected to the salt fog cabinet or to prolonged immersions in NaCl solutions is shown in Fig. 10. This figure shows that there is no significant deterioration of the surface, which maintains the same structure as before the corrosion process. This validates the synergistic protection properties of the silanes and polypyrrole coatings on the AA2024 surface, during its immersion in NaCl solutions.

The polarisation curves for coatings where polypyrrole was first electrodeposited and then the silane layer adsorbed (AA2024/Ppy/silane) are shown in Fig. 11. The electrochemical responses shown in this figure are very similar to those shown in Figs. 7, 9. Here, it can be seen that the effect is very similar to that of AA2024/silane/Ppy layers, i.e. the deposits with shorter adsorbed silane chains present the best anticorrosive behaviour, with more positive $E_{corr}$ and lower current values. One possible reason for this is that short chains adhere to the Ppy surface, plugging the small intergranular pores and creating an important barrier effect. This effect diminishes as the chain increases in size, and the longest chain produces the smallest effect on the anticorrosive property capacity, with the films being much less adherent and homogeneous.

### 3.2.3 *Electrochemical impedance measurements*

The EIS technique has been widely used to evaluate the corrosion resistance of coated metals. EIS measurements versus immersion time in 3% NaCl solution were taken for AA2024/$Al_2O_3$, AA2024/silane/Ppy and AA2024/Ppy/silane substrates, using the C3 silane coating. Figure 12 shows the impedance diagrams obtained for modified AA2024 electrodes at 24 and 360 h of immersion. For AA2024/$Al_2O_3$ (Fig. 12a and b), an increase is observed in impedance values as a function of immersion time, which may indicate an increase in aluminium oxide thickness and/or the formation of a more homogeneous film. In the Nyquist plot for 24 h (Fig. 12a), the formation of two capacitive semicircles from intermediate to low frequency regions is evident; meanwhile, for 360 h, only a broad maxima is observed. In Bode diagrams (phase angle versus frequency, Fig. 12b), various well-defined regions are observed, which can be related to the presence of different time constants; i.e. for 24 h, the presence of two maxima at 10 and 0.1 Hz, respectively, can be associated with the presence of two steps occurring simultaneously. The formation of these maxima for 360 h is poorly defined; however, the capacitive behaviour (at least in four decades) suggests an overlapping of these time constants. It is important to note, that Bode diagrams are more sensitive to elucidate different steps occurring simultaneously. In Fig. 12b it can be detected a small increase in angle values at the high frequency region from 10,000 to 1,000 Hz, approximately. Depending of the coating formed on AA2024, it can be observed different phase angle values. In this way, when exist only the

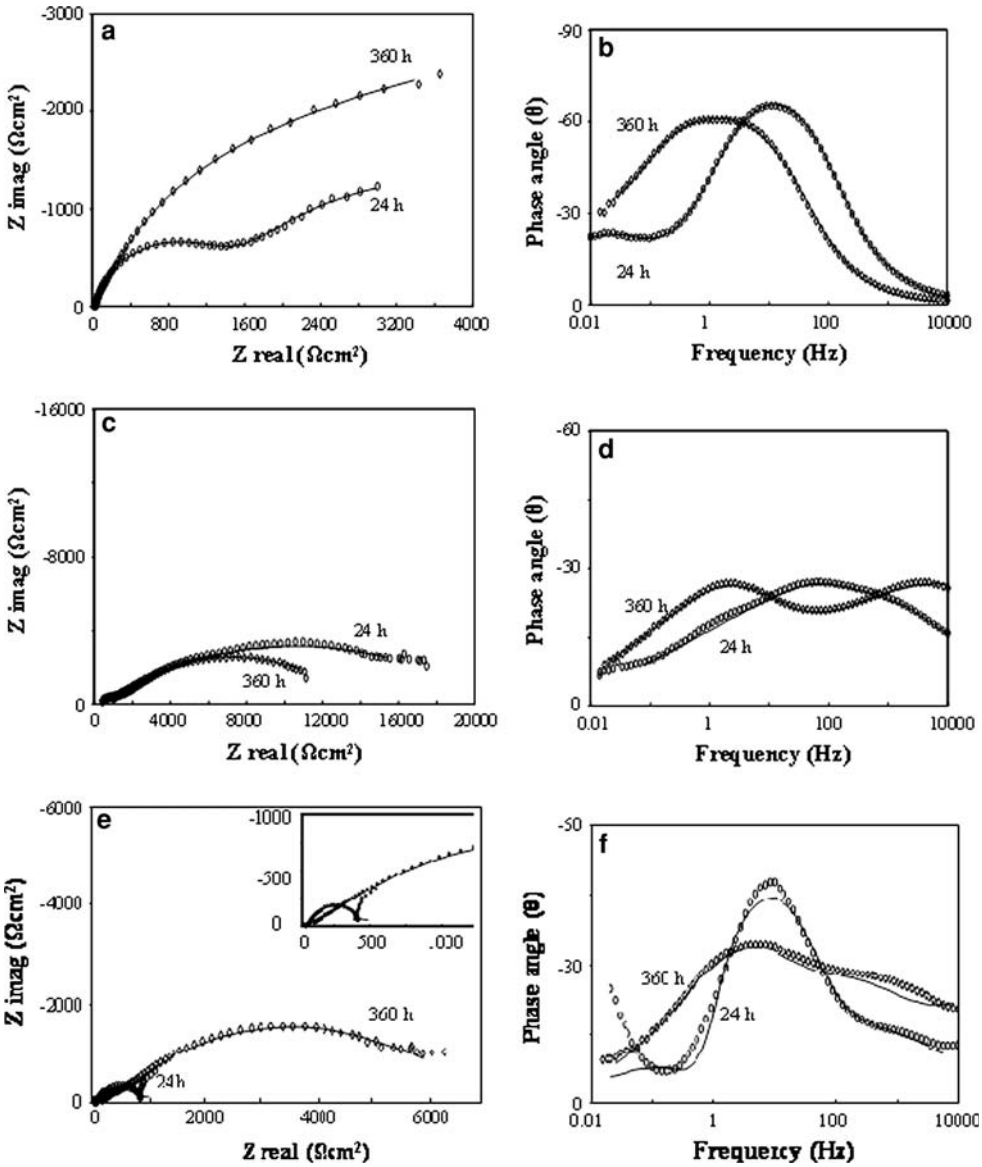


**Fig. 12** EIS diagrams obtained for AA2024 in 3% NaCl at 24 and 360 h: **a** and **b** AA2024/$Al_2O_3$, **c** and **d** AA2024/silane/Ppy, **e** and **f** AA2024/Ppy/silane. Continuous line corresponds to the fitting procedure using the equivalent circuit shown in Fig. 13

formation of an oxide–hydroxide aluminium, the angles obtained are smaller in comparison with those evaluated in Fig. 12d and f. This fact indicates the presence of a third time constant.

With regard to the coating effect, Fig. 12c and d show EIS diagrams for AA/silane/polypyrrole in NaCl at 24 and 360 h of immersion. In these figures, it is interesting to note that the impedance values are higher for AA2024/silanes/Ppy than for AA2024/$Al_2O_3$ and AA2024/Ppy/silanes (Fig. 12a and e) at 24 and 360 h of immersion. This suggests that the coating on the AA2024 is protective against the corrosion process throughout the immersion time, probably due to the formation of a homogeneous film and a less porous surface (acting mostly as a physical barrier). This is in agreement with the SEM image shown in Fig. 10, presenting the characteristics of the coating using the methodology described in the experimental section.

On the other hand, Nyquist diagrams show a similar response over immersion time of AA2024/silane/Ppy electrodes in sodium chloride, with the main difference being a decrease in impedance values at low frequencies for 360 h. In contrast, Bode diagrams show variations of phase angle values versus frequency. These variations are related to slight modifications of the coating previously formed on the anodised aluminium after the immersion, in agreement with the SEM image shown in Fig. 10. Moreover, the Bode diagrams show the presence of three time constants for all frequencies, as was suggested above. Also it can be observed an important increase of the phase angle values at high frequencies region (Fig. 12d), which corroborate the presence of the coating on AA2024.

The EIS diagrams recorded for the AA2024/Ppy/silanes immersed in NaCl solution (Fig. 12e and f) show greater modifications in the spectra than those observed for AA2024/$Al_2O_3$. These modifications in EIS diagrams may be related to modifications of surface conditions of the AA2024/Ppy/silanes over the immersion time. The low impedance values observed in the Nyquist plot at 24 h indicate an active surface of the AA2024, probably due to partial removal of the coating. This active condition favours a dissolution process of the AA2024, which indicates the presence of inductive behaviour poorly defined at low frequencies. This means that preparation of the Ppy/silane coating on a freshly polished aluminium surface is not the best way to ensure good adherence on the substrate. However, after 360 h of immersion, oxidation of the aluminium appears to be occurring, which reduces the active area of the AA2024 exposed to the aqueous solution. This causes the formation of aluminium oxides on the surface, which have a porous nature given the impedance magnitudes.

The formation of three time constants is observed in the characterisation of AA2024, in absence and/or presence of the various coatings. As a first approach, EIS analysis is carried out using the equivalent circuit shown in Fig. 13, which takes into consideration the presence of three steps occurring simultaneously. According to this equivalent circuit, Rs is the solution resistance, $Q_C$ and $R_C$ are the capacitance and resistance of the coating, respectively, which, in the case of anodised aluminium, are related to the previously formed oxide properties. $Q_{dl}$ and $R_{ct}$ are double layer capacitance and charge transfer resistance, respectively, of the non-covered regions of the aluminium in contact with the aqueous solution. The arrangement ($Q_d$-$R_d$) is used to describe the impedance response of molecular oxygen diffusion through the corrosion films formed on the AA2024. For the EIS plot obtained at 24 h for the AA/PP/silane coating, an L element was used instead of a $Q_d$-$R_d$ arrangement, to consider inductive response at low frequencies.

Fitting of the EIS diagrams is represented by the continuous line in Fig. 12, ensuring the quality of the simulation using the equivalent circuit shown in Fig. 13 and the program developed by Boukamp [35]. It is noteworthy that the fitting was poor only at the low-frequency region for the EIS plot obtained at 24 h for the AA2024/Ppy/silane coating, because the active behaviour of the electrode made the simulation difficult. However, most of the parameter values obtained in the simulation of the EIS experimental diagrams can be discussed. Table 1 summarises the electric parameter values obtained by the best fitting of the experimental data, where the $R_s$ values are not listed, given the small variation over immersion time. The pseudocapacitance values shown in Table 1 were evaluated using the following expression: C = ((Yo*R)^(1/n))/R [36]. The terms $Y_{o,C}$, $Y_{o,dl}$ and $n_C$, $n_{dl}$ were obtained using a constant phase element ($Q_c$ and $Q_{dl}$).

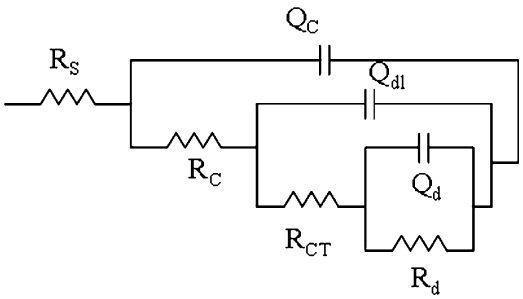


**Fig. 13** Equivalent circuit used for fitting the EIS diagrams shown in Fig. 12

Pseudocapacitance values (C) related to the corrosion products formed on the Al 2024 in absence and presence of different coatings immersed in 3% NaCl show greater variations mainly for the AA2024/$Al_2O_3$. The values obtained for AA2024/$Al_2O_3$ increase from 56 to 1110 μF, which is typical of the formation of aluminium oxides with a porous nature and non-protective properties [37]. Contrary to this finding, in presence of the coatings AA2024/silane/Ppy and AA2024/Ppy/silane, there is a decrease in capacitance values over immersion time, where the decrease is more dramatic in the case of AA2024/Ppy/silane. This variation can be related to a modification of the extent of coating coverage previously formed on the aluminium, which is more important for the AA2024/Ppy/silane. The capacitance values obtained in presence of the coatings are also worthy of note, suggesting the formation of a modified aluminium oxide film. Concerning double layer capacitance, an increase in values is observed in the following order: AA2024/silane/Ppy < AA2024l/Ppy/silane < AA2024/$Al_2O_3$. The values obtained for AA2024/Ppy/silane and AA2024/$Al_2O_3$ could be associated with an increase in the non-covered surface of the aluminium, as compared to AA2024/silane/Ppy.

Resistance values associated with the coating ($R_C$) are higher for AA2024/silane/Ppy, which corroborates the presence of the coating on the aluminium substrate; meanwhile, the charge transfer resistance of this coating is smaller when compared to the AA2024 and the Ppy coating. Finally, the increase in the resistive element related to molecular oxygen diffusion for AA2024/silane/Ppy suggests the formation of more homogeneous corrosion films when compared to the AA2024 and the Ppy coating. These results are supported by the SEM characterisation shown in Fig. 10, where one can observe the morphology of the films formed after the immersion of the AA2024/silane/Ppy.

## 4 Conclusions

The results obtained in this study show that the adsorption of organosilane layers of different chain sizes on a

**Table 1** Values of the electrical parameters obtained after simulation of the experimental impedance diagrams, using the equivalent circuit in Fig. 13 and the Boukamp program

| Tiempo (days) | $R_s$ (Ω) | $C_C$ (μF) | $R_c$ (Ω) | $C_{dl}$ (μF) | $R_{tc}$ (Ω) | $Q_d$ | | $R_d$ (Ω) |
|---|---|---|---|---|---|---|---|---|
| | | | | | | $Y_0 \times 10^{-3}$ (mho $s^n$) | $n$ | |
| $Al/Al_2O_3$ | | | | | | | | |
| 1 | 8.7 | 56 | 5.7 | 99.7 | 752.9 | 4.45 | 0.66 | 2,065.1 |
| 15 | 13.8 | 1,110 | 1,639.4 | 390.7 | 916.72 | 6.42 | 0.94 | 1,236 |
| Al/Ppy/silanes | | | | | | | | |
| 1 | 17.5 | 41.3 | 69.2 | 37.8 | 491.2 | | | 115.0[a] |
| 15 | 40 | 0.15 | 35.2 | 20.4 | 788.8 | 0.06 | 0.73 | 2,654.3 |
| Al/silanes/Ppy | | | | | | | | |
| 1 | 328 | 20 | 3,515.3 | 1.0 | 1,056.7 | 0.11 | 0.40 | 5,320.8 |
| 15 | 39.1 | 1.2 | 1,319.9 | 0.75 | 88.2 | 0.014 | 0.88 | 5,545.3 |

[a] This value corresponds to the L element, using for the simulation of this case

previously oxidised AA2024 surface produces good anchoring of electrochemically grown polypyrrole films. The corrosion behaviour of these films was tested in 3% NaCl solutions, with a corrosion potential that, in some cases, was up to 700 mV more positive than that of the AA2024 electrode coated with an oxide layer. The Ppy films that presented the best results were those electrodeposited on the silanes with the shortest chains. The substrates coated with a polypyrrole film upon which an organosilane was subsequently adsorbed showed fair anticorrosive behaviour with the NaCl immersion solutions. All of the results point to the viability of these layers as an anticorrosive treatment, although studies of their durability and interaction between layers are needed and will be addressed in future work.

**Acknowledgements** This work was financed by MEC through CTQ2005-04469/BQU. The author is also grateful to CONACYT for the scholarship granted.

## References

1. Hinton RW (1991) Met Finish 89:55
2. Jie H, Tallman DE, Bierwagen GP (2004) J Electrochem Soc 151:B644
3. Biallozor S, Kupniewska A (2005) Synth Met 155:443
4. Brânzoi V, Pilan L, Golgovici F (2006) Mol Cryst Liq Cryst 446:305
5. Akundy GS, Rajagopalan R, Iroh JO (2002) J Appl Polym Sci 83:1970
6. Ocón P, Cristóbal AB, Herrasti P, Fatás E (2005) Corros Sci 47:649
7. Naoi K, Takeda M, Kanno H, Sakakura M, Shimada A (2000) Electrochim Acta 45:3413
8. Martins NCT, Moura e Silva T, Montemor MF, Fernandes JCS, Ferreira MGS (2008) Electrochim Acta 53:4754
9. Plueddemann EP (1990) Silane coupling agents, 2nd edn. Plenum Press, New York
10. Franquet A, Terryn H, Le Pen C, Vereecken J (2001) Characterization of protection behaviour of aluminium alloys by silane coatings. In: Proceedings of EUROCORR, Riva del Garda, Italy, Milan (I), AIM, September 30–October 4, 2001, CD-ROM
11. Duarte R, Cabral AM, Montemor MF, Fernandes JCS, Ferreira MGS (2002) Keynote: environmentally friendly pre-treatments for aluminium alloys. In: Proceedings of the 15th International Corrosion Congress, Granada, Spain, September 22–27, CD-ROM
12. Frignani A, Zucchi F, Trabanelli G, Grassi V (2006) Corros Sci 48:2258
13. van Ooij WJ, Zhu D, Stacy M, Seth A, Mugada T, Gandhi J, Puomi P (2005) Tsinghua Sci Technol 10:639
14. Palanivel V, Zhu D, van Ooij WJ (2003) Prog Org Coat 47:384
15. Liu L, Ming Hu J, Qing Zhang J, Nan Cao C (2006) Electrochim Acta 52:538
16. Palanivel V, Huang Y, van Ooij WJ (2005) Prog Org Coat 53:153
17. Lamaka SV, Zheludkevich ML, Yasakau KA, Montemor MF, Ferreira MGS (2007) Electrochim Acta 52:7231
18. Saidman SB, Bessone JB (2002) J Electroanal Chem 521:87
19. Saidman SB, Quinzani OV (2004) Electrochim Acta 50:127
20. Breslin CB, Fenelon AM, Conroy KG (2005) Mat Des 26:233
21. Herrasti P, del Rio AL, Recio J (2007) Electrochim Acta 52:6496
22. Zhu D, Van Ooij WJ (2002) J Adhesion Sci Technol 16:1235
23. Song J, Van Ooij WJ (2003) J Adhesion Sci Technol 17:2191
24. Woo H, Reucroft PJ, Jacob RJ (1993) J Adhesion Sci Technol 7:681
25. Ono S, Saito M, Asoh H (2005) Electrochim Acta 51:827
26. Mazhar AA, Ei-Taib Heakal F, KhM Awad (1991) J Mater Sci 26:3707
27. Pancholi A, Stoleu VG, Kell CD (2007) Nanotechnology 18:5607
28. Jakobs RCM, Janssen LJJ, Barendrecht E (1985) Electrochim Acta 30:1433
29. Hülser P, Beck F (1990) J Appl Electrochem 20:596
30. Cecchetto L, Denoyelle A, Delabouglise D, Petit JP (2008) Appl Surf Sci 254:1736
31. Arenas MA, González Bajos L, de Damborenea JJ, Ocón P (2008) Prog Org Coat 62:79
32. Franquet A, Le Pen C, Terryn H, Vereechen J (2003) Electrochim Acta 48:1245

33. Herrasti P, Ocón P (2001) Appl Surf Sci 172:276
34. Boukamp BA (1993) Users manual equivalent circuit, version 4.51. Faculty of Chemical Technology, University of Twente, The Netherlands
35. Pech-Canul MA, Chi-Canul LP (1999) Corrosion 55:948
36. Bonnel A, Dabosi F, Deslouis C, Duprat M, Keddam M, Tribollet B (1983) J Electrochem Soc 130:753
37. Paloumpa I, Yfantis A, Hoffmann P, Burkov Y, Yfantis D, Schmeiber D (2004) Surf Coat Technol 180:308